23PM3D-03

Solving Optical Waveguide Leaky Modes Using a Multidomain Legendre Pseudospectral Frequency-Domain Method

Chih-Yu Wang [#1], Shih-Yung Chung [#2], Chun-Hao Teng [*3], Chung-Ping Chen [#4], Hung-chun Chang [†5]

[#] *Graduate Institute of Electronics Engineering and Department of Electrical Engineering, National Taiwan University, Taipei, Taiwan 10617, R.O.C.*
[1] d95943034@ntu.edu.tw [2] d95943006@ntu.edu.tw [4] cchen@cc.ee.ntu.edu.tw

[*] *Department of Applied Mathematics, National Chiao Tung University, Hsinchu, Taiwan 30010, R.O.C.*
[3] chunhao.teng@gmail.com

[†] *Department of Electrical Engineering, Graduate Institute of Photonics and Optoelectronics, and Graduate Institute of Communication Engineering, National Taiwan University, Taipei, Taiwan 10617, R.O.C.*
[5] hcchang@cc.ee.ntu.edu.tw

***Abstract*— A Legendre pseudospectral frequency-domain (PSFD) method incorporated with stretched coordinate perfectly matched layers (PMLs) and a multidomain technique is established for solving optical waveguide leaky modes. A recently developed penalty scheme is employed to assure numerical accuracy. This high-accuracy solver is used to analyze a leaky six-air-hole microstructured fiber, for which self convergence of accuracy in calculated effective indexes is demonstrated to be on the orders of 10^{-14}. Then, the photonic wire is analyzed and the comparison with the analysis results from other methods is discussed.**

I. Introduction

Some lately developed optical waveguides have confinement-loss characteristic, such as the microstructured fibers or photonic crystal fibers [1] and the photonic wire waveguide [2], and thus possess leaky modes having complex propagation constants. To solve such modes, a computational method needs to be implemented with well-functioning absorbing mechanism such as using the perfectly matched layers (PMLs) [3]. In optical waveguide analysis, the effective index, n_{eff}, which is defined as the propagation constant divided by the free-space wavenumber is usually chosen as an indicator for assessing the computation accuracy of a method. Different numerical methods for solving leaky modes have been developed, such as the more popular finite difference method and the finite element method. More recently, the pseudospectral frequency-domain (PSFD) methods [4], [5] have been proposed. This paper concerns further development of the pseudospectral method which is based on the high-order Legendre or Chebyshev interpolation basis and can then provide exponentially converged computation accuracy with respect to the grid resolution [6]. Prior PSFD mode solvers have been formulated using second-order Helmholtz equations [4]–[6] and demonstrated to provide excellent numerical accuracy in eigenmode analysis.

Recently, an alternate PSFD method with a penalty scheme was developed [7], which shows 10^{-15} accuracy in solving the modal effective indexes for standard metallic and fiber waveguides. Different from above-mentioned Helmholtz equations-based methods, this newly reported PSFD method is formulated on the first-order differential equations written from both curl and divergence laws in Maxwell's equations [8]. Besides, the multidomain scheme is employed in the formulation, with which the computational domain is divided into suitable number of curvilinear sub-domains [9] such that the shapes of the waveguide structure interfaces can fit the sub-domain boundaries, facilitating accurate fulfillment of the field continuity conditions across the interfaces. In this paper, this new method is adopted and implemented with the stretched coordinate PML [3], which is quite suitable for first-order equations, for solving waveguide leaky modes with high accuracy. We will show in the numerical examples that the inclusion of the stretched coordinate PML still maintains high accuracy of the PSFD method. The governing Maxwell's equations with the penalty scheme, the implementation of the stretched coordinate PML, and the eigenmode solver formulation are described in Section II. The Legendre pseudospectral method is introduced in Section III. Then, numerical examples containing the six-air-hole fiber and the photonic wire are given and discussed in Section IV. The conclusion is drawn in Section V.

II. Maxwell's Equations, PML, and Penalty-Scheme Formulation

We consider source-free and linear isotropic medium with permittivity ε and permeability μ, and the time-harmonic problem at the angular frequency ω for frequency-domain computation. Waves are considered to propagate along the z-axis in a waveguide with no structural variations along the z direction. Therefore, spatial derivative with respect to z becomes $\partial/\partial z = -j\beta$, where β is the modal propagation constant. For convenience, we normalize the magnetic field $\mathbf{H}$ to $\sqrt{\varepsilon_0/\mu_0}\mathbf{H}$. In the pseudospectral multidomain formulation, the whole computational domain is divided into sub-domains, including the PML regions. Each PML sub-domain represents

the most general sub-domain as far as the the expressions for the governing equations are concerned. Consider two adjacent PML sub-domains I and II, with the unit normal vector $\hat{n} = n_x\hat{x} + n_y\hat{y}$ perpendicular to the interface between with the relationship $\hat{n} = \hat{n}^I = -\hat{n}^{II}$, where the superscripts I and II specify the sub-domains where the vectors are defined at the interface. The boundary conditions at this interface is treated using a penalty scheme as in [7]. We can obtain the following six first-order equations involving the six electric and magnetic field components:

$$-jk_0H_y^I + \frac{1}{s_x}\frac{\partial E_z^I}{\partial x} - \frac{\delta}{2\omega_0}\frac{n_x^I}{s_x}(E_z^I - E_z^{II}) = j\beta E_x^I \quad \text{(1a)}$$

$$jk_0H_x^I + \frac{1}{s_y}\frac{\partial E_z^I}{\partial y} - \frac{\delta}{2\omega_0}\frac{n_y^I}{s_y}(E_z^I - E_z^{II}) = j\beta E_y^I \quad \text{(1b)}$$

$$-\frac{1}{s_x}\frac{\partial E_x^I}{\partial x} - \frac{1}{s_y}\frac{\partial E_y^I}{\partial y} + \frac{\delta}{2\omega_0}[\frac{n_x^I}{s_x}(E_x^I - \frac{\varepsilon_r^{II}}{\varepsilon_r^I}E_x^{II}) + \frac{n_y^I}{s_y}(E_y^I - \frac{\varepsilon_r^{II}}{\varepsilon_r^I}E_y^{II})] = j\beta E_z \quad \text{(1c)}$$

$$jk_0\varepsilon_r^I E_y^I + \frac{1}{s_x}\frac{\partial H_z^I}{\partial x} - \frac{\delta}{2\omega_0}\frac{n_x^I}{s_x}(H_z^I - H_z^{II}) = j\beta H_x^I \quad \text{(1d)}$$

$$-jk_0\varepsilon_r^I E_x^I + \frac{1}{s_y}\frac{\partial H_z^I}{\partial y} - \frac{\delta}{2\omega_0}\frac{n_y^I}{s_y}(H_z^I - H_z^{II}) = j\beta H_y^I \quad \text{(1e)}$$

$$-\frac{1}{s_x}\frac{\partial H_x^I}{\partial x} - \frac{1}{s_y}\frac{\partial H_y^I}{\partial y} + \frac{\delta}{2\omega_0}[\frac{n_x^I}{s_x}(H_x^I - H_x^{II}) + \frac{n_y^I}{s_y}(H_y^I - H_y^{II})] = j\beta H_z^I. \quad \text{(1f)}$$

In (1), δ is unity when the grid point is at the boundary edge, and is zero otherwise, and ω_0 is the quadrature weight on the interface which will be defined in the next section, s_x and s_y are the PML absorptive paramaters, and the terms with $\delta/(2\omega_0)$ are penalty terms. With $s_x = s_y = 1$ and all the penalty terms removed, (1) in fact becomes the six equations resulting from the eight component equations of the four time-harmonic Maxwell's curl and divergence equations. Two of the eight equations are without $j\beta$ terms and are not included. The derivation of the penalty terms was discussed in [7].

The six equations in (1) lead to an eigen-problem in the form, $\tilde{A}\tilde{x} = \lambda\tilde{x}$, for solving waveguide modes, with $\tilde{A}$ containing the differential operators, the eigenvalue λ equal to $j\beta$ to be searched, and the eigenvector $\tilde{x}$ composed of the electric and magnetic fields of the corresponding mode. This eigen-problem can be solved using efficient iterative algorithms such as the bi-conjugate gradient (BiCG) method along with the shifted inverse power method (SIPM).

For solving waveguide leaky modes, a suitable perfectly matched layer (PML) is required to be implemented. The stretched coordinate PML [3] is chosen in this paper because of its ease of implementation on first order equations and its outstanding ability of absorbing outward propagating waves. According to [3], the stretched coordinate PML can be implemented by simply changing partial derivatives as $\partial/\partial\tilde{x} = (1/s_x)\partial/\partial x$ and $\partial/\partial\tilde{y} = (1/s_y)\partial/\partial y$. Similarly, the vector differential operator $\tilde{\nabla}$ in the stretched coordinate becomes $\tilde{\nabla} = \tilde{x}(1/s_x)\partial/\partial x + \tilde{y}(1/s_y)\partial/\partial y$. The absorptive variables s_x and s_y are defined as $s_x = 1 + \frac{\sigma_x}{j\omega\varepsilon}$ and $s_y = 1 + \frac{\sigma_y}{j\omega\varepsilon}$ [3], where σ_x and σ_y are the electric conductivities. To reduce possible undesired reflection waves, we choose suitable profiles for σ_x and σ_y such as, for example, $\sigma_x(x_i) = c(\frac{|x_i - x_0|}{L_{PML}})^m$ along the x-axis, with the parameters c and m being free variables for adjusting performance of the PML, $|x_i - x_0|$ is the distance of the ith grid point away from the innermost interface of the PML, and L_{PML} is the length of the PML region. This is a gradually and exponentially growing profile and thus its strength of absorption as the grids get deeper into the PML region. Generally, the PML is designed to absorb waves in a single direction, therefore similar σ_y profile along the y direction is used by replacing the variable x with y in $\sigma_x(x_i)$, and both σ_x and σ_y will be needed at the corner region of the PML.

III. The Legendre Pseudospectral Method Formulation

Now we discuss the Legendre pseudospectral method for numerically treating the spatial derivatives in the above governing equations. Under the multidomain scheme, each curvilinear quadrilateral sub-domain region in Cartesian coordinates (x, y) can be mapped onto a square region $[-1, 1] \times [-1, 1]$ in curvilinear coordinates (ξ, η) by using the transfinite blending function described in [9] to construct $\xi = \xi(x, y)$ and $\eta = \eta(x, y)$.

In the Legendre pseudospectral method, spatial arrangement of grid points is defined by the Legendre-Gauss-Lobatto (LGL) quadrature points ξ_i arranged in the interval $[-1, 1]$, which are the roots of the polynomial $(1 - \xi^2)P'_N(\xi)$ [6], [7] with the prime denoting derivative and P_N being the Legendre polynomial of degree N defined by

$$P_N(\xi) = \frac{1}{2^N N!}\frac{d^N}{d\xi^N}(\xi^2 - 1)^N\,. \quad (2)$$

Associated with these LGL quadrature points are a set of quadrature weights ω_i for $i = 0, 1, 2, \ldots, N$. If $f(\xi)$ is a polynomial of degree at most $2N - 1$, we have the quadrature rule [6], [7]: $\sum_{i=0}^{N} f(\xi_i)\omega_i = \int_{-1}^{1} f(\xi)d\xi$, where the quadrature weights are defined as $\omega_i = 2/[N(N+1)]$ when $i = 0, N$, and $\omega_i = -\{2/(N + 1)\}\{1/[P_N(\xi_i)P'_{N-1}(\xi_i)]\}$, otherwise. Based on these LGL collocation points, one can use the degree-N Lagrange interpolation polynomials $l_j(\xi)$ as the bases to approximate an arbitrary function $f(\xi)$ such that

$$f(\xi) \approx \sum_{j=0}^{N} f(\xi_j)l_j(\xi) \quad (3)$$

where

$$l_j(\xi) = -\frac{(1 - \xi^2)P'_N(\xi)}{N(N + 1)(\xi - \xi_j)P_N(\xi_j)}\,. \quad (4)$$

Then, the derivative of the function $f(\xi)$ at the LGL quadrature point ξ_i can also be approximated as

$$\frac{df(\xi_i)}{d\xi} \approx \sum_{j=0}^{N}\frac{dl_j(\xi_i)}{d\xi}f(\xi_j) = \sum_{j=0}^{N} D_{ij}f(\xi_j)\,. \quad (5)$$

The differential coefficient D_{ij} is defined in [6] and [7] by

$$D_{ij} = \begin{cases} -\frac{N(N+1)}{4}\,, & i = j = 0 \\ \frac{N(N+1)}{4}\,, & i = j = N \\ 0\,, & 0 < (i = j) < N \\ \frac{P_N(\xi_i)}{P_N(\xi_j)}\frac{1}{\xi_i - \xi_j} & i \neq j. \end{cases} \quad (6)$$

The matrix with D_{ij} elements is called the differential matrix operator. This is the key feature of the Legendre PSFD method, i.e., for the 1-D example, the derivative of $f(\xi)$ at an LGL point ξ_i in the region $[-1, 1]$ can be approximated in terms of $f(\xi)$ values at the $N + 1$ LGL points in the same region. Therefore, spatial derivatives of fields in (1) can be simply replaced by this differential matrix operator D_{ij} in the $\tilde{A}\tilde{x} = \lambda\tilde{x}$ eigen-problem system, and the resultant eigen-problem becomes a sparse matrix having penalty, PML, and repeatedly appearing D_{ij} terms in the $\tilde{A}$ matrix.

In the 2-D waveguide structures to be discussed in the next section, the grid meshes based on the LGL points in each sub-domain will be plotted for a given $N = 10$. In the figures showing grid meshes, the curved structure and the whole computational region can be seen being partitioned into curvilinear sub-domains, and $(N + 1) \times (N + 1)$ LGL grid points are not uniformly distributed but somewhat following the outline of the domain edges. Please note that the LGL grid points at each edge side of a sub-domain are co-located with the LGL grid points at one edge side of its adjacent sub-domain. These co-located grid points are counted as distinct sets of points, and the penalty scheme is applied on the two sets for exchanging information of boundary conditions.

IV. Numerical Results

In this section, we will apply our PSFD method with stretched coordinate PML to solve the microstructured six-air-hole fiber [10], [11] and the photonic wire waveguide [2]. The latter is with sharp dielectric corners at which electric-field singularities might exist.

The cross-section of the six-air-hole fiber is depicted in Fig. 1(a). With the structural symmetry, we can treat only one quarter of the waveguide cross-section. Domain partitioning and grid meshes in the computation are shown in Fig. 1(b). The PML, not shown in Fig. 1(b), is designed to be in the region ($x \geq 10\,\mu$m and $y \geq 10\,\mu$m). According to [5] and [10], six holes are hexagonally arranged, and the hole pitch, i.e., the center-to-center distance of adjacent holes, is $\Lambda = 6.75\,\mu$m. The radius of each hole is $R = 2.5\,\mu$m, and the refractive indexes for the fiber and the hole are $n = 1.45$ and 1.0, respectively. The $p = 1$ and $p = 3$ modes, as defined in [10], are considered here at $\lambda = 1.45\,\mu$m. The PSFD computed complex effective indexes for these two modes are $1.438364934178884 + j0.000001416475997$ and $1.445395232149295 + j0.000000031945250$, respectively, when $N = 16$ is used. Accuracy of self-convergence on the order of 10^{-14} is observed for this complicated structure, referring to the $N = 16$ results. According to the result of the multipole method proposed in [10], the computed effective index for this $p = 1$ mode was $n_{eff} = 1.43836493424529 + j0.00000141647574$, which agrees well with our results to 10^{-9} for the real part and to 10^{-12} for the imaginary part. On the other hand, a new high-order boundary-integral-equation (BIE) method was reported recently and shown to achieve exponential convergence and extremely high accuracy [11]. The computed effective index for the $p = 3$ mode provided in [11] is $n_{eff} = 1.4453952321493 + j0.00000003194529$, which agrees with our results to the order of 10^{-13} for both the real and imaginary parts. The PSFD computed electric mode-field distributions are shown in Fig. 2(a)–(c) for the $p = 1$ mode and in Fig. 3(a)–(c) for the $p = 3$ mode. The errors of the PSFD calculated n_{eff}s versus N for the $p = 1$ and $p = 3$ modes are plotted in Fig. 1(c) to show the characteristics of numerical convergence of the developed PSFD mode solver. For each N, the error of n_{eff} is defined as the absolute value of the difference between the calculated n_{eff} and that obtained using $N = 16$. Fig. 1(c) is presented in logarithmic scales, and exponential convergence of computational accuracy is observed, which means that numerical errors can be fast reduced by a relatively small increase in the number of grid points.

The photonic wire waveguide or photonic wire has been an essential structure in recently developed high-density photonic integrated circuits, and the computed effective indexes of its fundamental mode have been compared among ten different numerical methods or solvers in [2]. As shown in the inset of Fig. 4(a), the guiding core and the substrate are both made of silicon with $n = 3.5$ and there is a SiO_2 buffer layer between them with $n = 1.45$. The upper cover medium is air, resulting in a high-index-contrast structure. The rectangular core has of course sharp corners. One important characteristic is that the limited thickness of the SiO_2 buffer causes the fundamental mode to leak power into the substrate, and the accurate determination of Im[n_{eff}] becomes a main concern. To compare with the results in [2], we adopt the same parameters: the width and the height of the core being $0.5\,\mu$m and $0.22\,\mu$m, respectively, the thickness of the buffer layer being $1.0\,\mu$m, and $\lambda = 1.55\,\mu$m. The designed sub-domain arrangement for half structure is shown in Fig. 4(b). The PML regions (not shown) are put outside the right, bottom, and top sides with thicknesses $4\,\mu$m, $4\,\mu$m, and $2\,\mu$m, respectively. The PSFD computed complex effective indexes are for different Ns up to 32. We would have confidence that Re[n_{eff}] = 2.412374 (order of 10^{-6} accuracy) and Im[n_{eff}] = 2.91×10^{-8} (order of 10^{-10} accuracy), but showing relatively slow convergent rate for this high-index-contrast structure with corners.

It was shown in [2] that the agreement between the film mode matching method and the aperiodic fourier modal method was the best with the agreement for Re[n_{eff}] on seven significant digits and for Im[n_{eff}] on five significant digits after rounding. It is found that our PSFD result agrees with these two methods on six significant digits for Re[n_{eff}] (2.41237) and on three digits for Im[n_{eff}] (2.91×10^{-8}). Fig. 4(a) shows the Re[E_x] profile along the y-axis at $x = 0$ together with the waveguide refractive-index profile. The mode field is seen mostly guided in the core, decaying in the SiO_2 buffer layer, leaking into the Si substrate, and absorbed by the PML layer. The PML is placed at $y < 4\,\mu$m (substrate). The PSFD calculated $|E_x|$, $|E_y|$, and $|E_z|$profiles for the fundamental mode are shown in Fig. 5(a)–(c), respectively. The field singular points can be seen in Fig. 5(b).

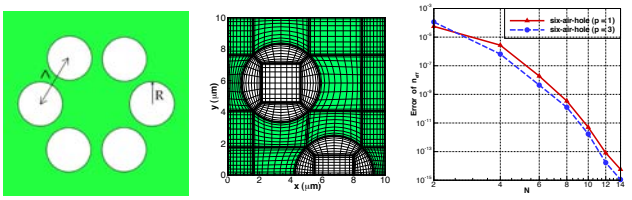

(a) (b) (c)

Fig. 1: (a) Cross-section of the six-air-hole fiber. (b) Illustration of the sub-domain arrangement and grid mesh. (c) Exponential convergence characteristics of the error of n_{eff} versus N.

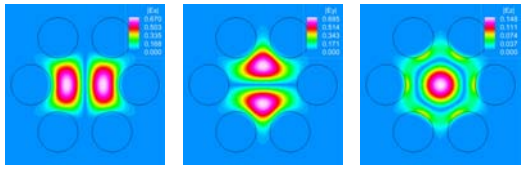

(a) (b) (c)

Fig. 2: Field profiles of the $p = 1$ mode of the six-air-hole fiber waveguide. (a) $|E_x|$. (b) $|E_y|$. (c) $|E_z|$.

V. Conclusion

We have incorporated the stretched coordinate PMLs into the recently developed pseudospectral frequency-domain (PSFD) method waveguide mode solver which employs a penalty scheme [7] so that leaky modes can be determined with high-accuracy complex effective indexes. Applications of the new PSFD solver to the popularly studied microstructured six-air-hole fiber demonstrates self convergence of accuracy in the effective index on the order of 10^{-14} is achieved. For the high-index-contrast photonic wire with substrate leakage, the PSFD solver provides an effective index for the fundamental mode close to the possible best results offered by the film mode matching method and the aperiodic fourier modal method among ten methods compared in [2] with the agreement on six significant digits for the real part and on three digits for the imaginary part.

Acknowledgements

This work was supported in part by the National Science Council of the Republic of China under grants NSC99-2221-E-002-107-MY2 and NSC99-2115-M-009-012-MY3, and in part by the Excellent Research Projects of National Taiwan University under grant 10R80919-1. The authors would like to thank the Computer and Information Networking Center at National Taiwan University for providing useful computing resources.

References

[1] P. St. J. Russell, "Photonic crystal fibers," *Science*, vol. 299, pp. 358–362, 2003.

[2] P. Bienstman, S. Selleri, L. Rosa, H. P. Uranus, W. C. L. Hopman, R. Costa, A. Melloni, L. C. Andreani, J. P. Hugonin, P. Lalanne, D. Pinto, S. S. A. Obayya, M. Dems, and K. Panajotov, "Modelling leaky photonic wires: A mode solver comparison," *Opt. Quantum Electron.*, vol. 38, pp. 731–759, 2006.

[3] W. C. Chew and W. H. Weedon, "A 3-D perfectly matched medium from modified Maxwell's equations with stretched coordinates," *Microwave Opt. Tech. Lett.*, vol. 7, pp. 599–604, Sep. 1994.

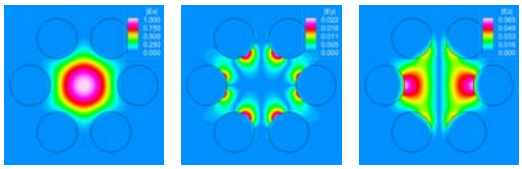

(a) (b) (c)

Fig. 3: Field profiles of the $p = 3$ mode of the six-air-hole fiber waveguide. (a) $|E_x|$. (b) $|E_y|$. (c) $|E_z|$.

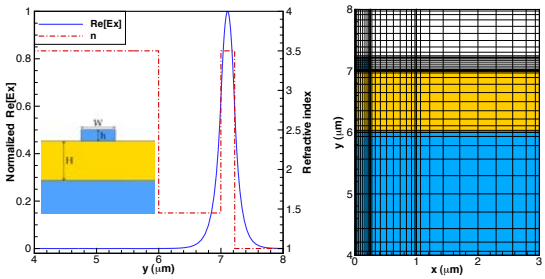

(a) (b)

Fig. 4: (a) Structural refractive-index profile along the y-axis at $x = 0$ and Re$[E_x]$ of the fundamental mode versus y distribution at $x = 0$ for the photonic wire waveguide. The inset shows the waveguide cross-section. (b) Illustration of the sub-domain arrangement and grid mesh.

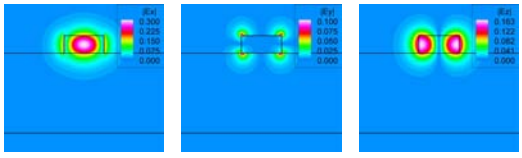

(a) (b) (c)

Fig. 5: Field profiles of the fundamental mode of the photonic wire waveguide. (a) $|E_x|$. (b) $|E_y|$. (c) $|E_z|$.

[4] C. C. Huang, "Numerical calculations of ARROW structures by pseudospectral approach with Mur's absorbing boundary conditions," *Opt. Express*, vol. 14, pp. 11631–11652, Nov. 2006.

[5] P. J. Chiang and H. C. Chang, "A high-accuracy pseudospectral full-vectorial leaky optical waveguide mode solver with carefully implemented UPML absorbing boundary conditions," *Opt. Express*, vol. 19, pp. 1594–1608, Jan. 2011.

[6] P. J. Chiang, C. L. Wu, C. H. Teng, C. S. Yang, and H. C. Chang, "Full-vectorial optical waveguide mode solvers using multidomain pseudospectral frequency-domain (PSFD) formulations," *IEEE J. Quantum Electron.*, vol. 44, pp. 56–66, Jan. 2008.

[7] S. F. Chiang, B. Y. Lin, H. C. Chang, C. H. Teng, C. Y. Wang, and S. Y. Chung, "A Multidomain Pseudospectral Mode Solver for Optical Waveguide Analysis," *J. Lightwave Technol.*, vol. 20, pp. 2077–2087, July 1, 2012.

[8] C. H. Teng, B. Y. Lin, H. C. Chang, H. C. Hsu, C. N. Lin, and K. A. Feng, "A Legendre pseudospectral penalty scheme for solving time-domain Maxwell's equations," *J. Sci. Comput.*, vol. 36, pp. 351–390, Sept. 2008.

[9] W. J. Gordon and C. A. Hall, "Transfinite element methods: Blending-function interpolation over arbitrary curved element domains," *Numer. Math.*, vol. 21, pp. 109–129, 1973.

[10] T. P. White, B. T. Kuhlmey, R. C. McPhedran, D. Maystre, G. Renversez, C. M. de Sterke, and L. C. Botten, "Multipole method for microstructured optical fibers. II. Implementation and results," *J. Opt. Soc. Amer. B*, vol. 19, pp. 2331–2340, Oct. 2002.

[11] W. T. Lu and Y. Y. Lu, "Efficient boundary integral equation method for photonic crystal fibers," *J. Lightwave Technol.*, vol. 30, pp. 1610–1616, June 1, 2012.